**OC-0214**

**Hybrid MLC and couch tracking**

J. Toftegaard[1], R. Hansen[1], K. Macek[2], P.R. Poulsen[1]
[1]*Aarhus University Hospital, Department of Oncology, Aarhus C, Denmark*
[2]*Varian Medical Systems, Imaging Laboratory, Baden, Switzerland*

**Purpose or Objective:** MLC and couch tracking are promising techniques for intrafractional tumor motion management. However, both techniques have their limitations that result in residual dosimetric errors: MLC tracking perpendicular to the MLC leaves is limited by the finite MLC leaf width, while couch tracking has slower dynamics than the MLC and might be uncomfortable for the patient. Here, we suggest a range of potential hybrid MLC-couch tracking strategies and test the performance of each strategy with extensive tracking simulations.

**Material and Methods:** Three hybrid MLC-couch tracking strategies were investigated and compared with pure MLC tracking and pure couch tracking. Dividing the target motion into motion parallel and perpendicular to the MLC leaves in beam's eye view, the investigated tracking strategies were as follows (in order or increasing MLC tracking fraction). 1) Pure couch tracking; 2) Couch for all perpendicular target motion and MLC for parallel motion; 3) Couch for perpendicular motion below one leaf width and MLC for the remaining motion; 4) Same as 3) except that the couch only adapts to stable perpendicular shifts with standard deviation below 0.5mm during the last second; 5) Pure MLC tracking.
The current developer release of TrueBeam tracking system does not allow for hybrid MLC-couch tracking, but our in-house built tracking simulator allowed investigation of the hybrid strategies. The simulator was experimentally validated to mimic the TrueBeam MLC and couch tracking system. Tracking treatments with each tracking strategy were simulated for 160 lung tumor and 695 prostate trajectories. A high and a low modulated VMAT treatment (1 arc) with MLC motion in the superior-inferior direction were simulated for each trajectory.
The tracking performance of each simulated treatment was quantified as the mean MLC exposure error in beam's eye view. The MLC exposure error is the sum of under-exposed areas Au (MLC shielded areas that should ideally be exposed) and over-exposed areas Ao (MLC exposed areas that should ideally be shielded). Au+Aohas previously been shown to be a good surrogate for dosimetric errors in tracking treatments.

**Results:** The figure shows the cumulative distribution of mean MLC exposure errors for all trajectories and for trajectories with large motion (>3mm for prostate, >5mm for lung).The table shows the median reduction in the exposure error relative to pure MLC tracking as well as the mean 3D couch speed for all tracking strategies.

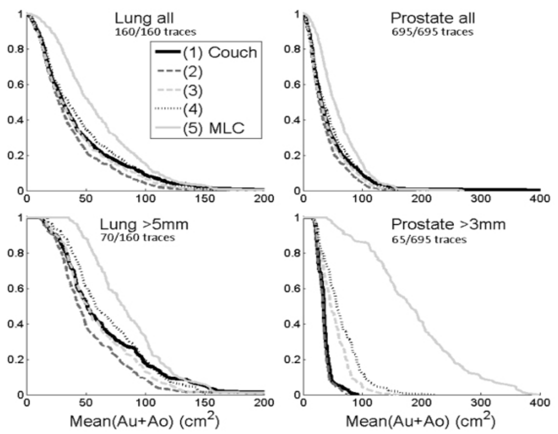


*Figure 1: Cumulative plot for Mean over- and under-exposed areas for each site. Upper figure are all traces and lower are only traces with motion more than 5mm (Lung) and 3mm (Prostate). Numbers in legend refer to numbers in methods.*

| | | Prostate | | Lung | |
|---|---|---|---|---|---|
| | | **all** | **>3mm** | **all** | **>5mm** |
| Exposure error | (1) Couch | 42.31% | 80.92% | 42.31% | 37.69% |
| | (2) | **48.78%** | **81.67%** | **48.78%** | **45.90%** |
| | (3) | 42.78% | 73.98% | 42.78% | 36.35% |
| | (4) | 33.94% | 68.57% | 33.94% | 29.05% |
| | (5) MLC | 0.00% | 0.00% | 0.00% | 0.00% |
| Motion | (1) Couch | 0.827 mm | 0.882 mm | 2.52 mm | 3 mm |
| | (2) | 0.741 mm | 0.86 mm | 1.84 mm | 2.34 mm |
| | (3) | 0.766 mm | 1.03 mm | 1.84 mm | 2.35 mm |
| | (4) | 0.67 mm | 0.809 mm | 1.07 mm | 1.17 mm |
| | (5) MLC | 0 mm | 0 mm | 0 mm | 0 mm |

*Table 1: Upper part: Median reduction in percent of mean exposure error relative to pure MLC tracking. Lower part: Average couch speed.*

**Conclusion:** Hybrid MLC-couch tracking offers a continuum of trade-offs between tracking accuracy and couch motion. A modest degree of couch tracking (strategy 4) largely improved MLC tracking, especially for prostate motion exceeding 3mm. Couch tracking perpendicular to the MLC leaves and MLC tracking parallel to the leaves (strategy 2) gave the most accurate tracking and a large couch motion reduction compared to pure couch tracking.

**OC-0215**

**Mapping of breathing and cardiac induced motion of lymph node targets in lung cancer patients**

M.L. Schmidt[1], L. Hoffmann[2], M. Knap[1], T.R. Rasmussen[3], B.H. Folkersen[3], J. Toftegaard[1], D.S. Møller[2], P.R. Poulsen[1]
[1]*Aarhus University Hospital, Department of Oncology, Aarhus C, Denmark*
[2]*Aarhus University Hospital, Department of Medical Physics, Aarhus C, Denmark*
[3]*Aarhus University Hospital, Department of Pulmonology, Aarhus C, Denmark*

**Purpose or Objective:** Malignant mediastinal lymph nodes (LNs) are often included in the planning target volume for lung cancer patients (pts), but LN motion is not well investigated and this may potentially undermine the locoregional control. LNs in the mediastinum are difficult to visualize in cone-beam CT (CBCT) scans. In this study, the position of implanted fiducial markers obtained from daily CBCT projections was used to map the 3D intrafraction and interfraction motion of LN targets throughout the treatment course for ten lung cancer pts.

**Material and Methods:** Ten lung cancer pts with Visicoil fiducial markers implanted in LN targets by EBUS bronchoscope received intensity modulated radiotherapy (RT) treatment in 30-33 fractions. A total of 26 LN targets with Visicoils were analyzed. A pre-treatment setup CBCT scan with ~675 projections was used for daily online soft tissue match on the primary tumor (GTV-T). The Visicoil positions were segmented offline in each projection using a semi-automatic template-based algorithm. From the segmented Visicoil positions the 3D Visicoil trajectories were estimated with 11Hz sample rate by a probability-based estimation method. By frequency analysis, the 3D trajectories were separated into a cardiac and a breathing component. The motion ranges of the Visicoils were extracted in the left-right (LR), cranial-caudal (CC) and anterior-posterior (AP) direction for the total motion, as well as the separated cardiac and breathing induced motions. Also, the daily mean setup error of the Visicoils after the GTV-T soft-tissue match was extracted and used to calculate motion margins required for interfraction baseline shifts of the LN targets (using the formula $2.5\Sigma+0.7\sigma$)*.

**Results:** The 2-98 percentile motion ranges, for the patient group were in mean (with standard deviation) 2.1mm (0.5mm)(LR), 7.3mm (2.6mm)(CC), 3.3 mm (1.3mm)(AP). The cardiac induced mean motion ranges were 1.3mm 0.7mm)(LR), 1.3mm (0.6mm)(CC), 2.3mm (1.5mm)(AP). The figure shows the averaged waveform in the coronal plane of the cardiac and breathing motion components of each Visicoil at the first RT fraction. The waveforms were obtained by averaging over a number of breathing/cardiac cycles.